Calcium Channel β Subunit Promotes Voltage-Dependent Modulation of α1B by G$\beta\gamma$

Alon Meir, Damian C. Bell, Gary J. Stephens, Karen M. Page, and Annette C. Dolphin
Department of Pharmacology, University College London, London WC1E 6BT, United Kingdom

ABSTRACT Voltage-dependent calcium channels (VDCCs) are heteromultimers composed of a pore-forming α1 subunit and auxiliary subunits, including the intracellular β subunit, which has a strong influence on the channel properties. Voltage-dependent inhibitory modulation of neuronal VDCCs occurs primarily by activation of G-proteins and elevation of the free G$\beta\gamma$ dimer concentration. Here we have examined the interaction between the regulation of N-type (α1B) channels by their β subunits and by G$\beta\gamma$ dimers, heterologously expressed in COS-7 cells. In contrast to previous studies suggesting antagonism of G protein inhibition by the VDCC β subunit, we found a significantly larger G$\beta\gamma$-dependent inhibition of α1B channel activation when the VDCC α1B and β subunits were coexpressed. In the absence of coexpressed VDCC β subunit, the G$\beta\gamma$ dimers, either expressed tonically or elevated via receptor activation, did not produce the expected features of voltage-dependent G protein modulation of N-type channels, including slowed activation and prepulse facilitation, while VDCC β subunit coexpression restored all of the hallmarks of G$\beta\gamma$ modulation. These results suggest that the VDCC β subunit must be present for G$\beta\gamma$ to induce voltage-dependent modulation of N-type calcium channels.

INTRODUCTION

VDCCs play an essential role in the control of many cellular processes, including synaptic transmission, by transducing a voltage signal into elevation of intracellular Ca^{2+} (Tsien et al., 1991; Dunlap et al., 1995). In presynaptic nerve terminals, the VDCCs that are most involved in transmitter release are N-type (α1B) and P/Q-type (α1A) channels (Meir et al., 1999). Many neurotransmitters, including dopamine, GABA, and opiates, are involved in a widespread form of inhibitory synaptic modulation, by binding to presynaptic seven transmembrane domain (7TM) receptors, liberating activated G protein subunits, and inhibiting calcium currents (Bean, 1989; Dolphin, 1995). This inhibition is produced by the G$\beta\gamma$ dimers, which associate with α1B VDCCs in particular (Ikeda, 1996; Herlitze et al., 1996) (but also with α1A and α1E), in a membrane-delimited manner, causing the channels to lose the property of fast opening in response to depolarization, so that less Ca^{2+} enters the cell. This modulation involves a retardation of the activation process of VDCCs (Carabelli et al., 1996; Patil et al., 1996), which can be overcome (voltage-dependent facilitation) by a strong depolarizing prepulse (Ikeda, 1991) or a train of action potentials (Patil et al., 1998). G protein modulation of VDCCs embeds three major elements: reduction of the current amplitude, slowing of the activation kinetics, and relief of inhibition by depolarizing voltages. Recent single-channel and gating current analysis has suggested that the modulation consists mainly of G$\beta\gamma$-bound channels failing to gate to the open state, implying a requirement that G$\beta\gamma$ unbinds before gating (adding this relatively slow component to the activation kinetics) (Patil et al., 1996; Jones et al., 1997). Therefore, it was proposed that the kinetic slowing alone caused the amplitude decrease. In this model, facilitation is explained by voltage-dependent unbinding of the modulating G protein during a strong depolarizing prepulse (Elmslie and Jones, 1994). However, other data suggest that "reluctant" or G$\beta\gamma$-bound calcium channels may also open (Elmslie et al., 1990; Boland and Bean, 1993; Colecraft et al., 2000).

VDCCs are heteromultimers composed of a pore-forming α1 subunit and several auxiliary subunits (Jones, 1998). The α1 subunits are the primary determinants of the resultant properties; however, the auxiliary subunits, particularly the intracellular β subunit, strongly influence the properties of the assembled channels (Walker and De Waard, 1998). VDCC β subunits (of which four isoforms have been cloned) are involved in membrane targeting of the putative pore-forming α1 subunits (Chien et al., 1995; Brice et al., 1997) and modulate the biophysical properties of α1C (Costantin et al., 1998; Gerster et al., 1999), α1E (Stephens et al., 1997), and α1B (Wakamori et al., 1999) channels. A common effect of the different β subunits is to enhance the coupling between depolarization and activation and to increase the channel open probability (for a review see Walker and De Waard, 1998).

There is biochemical evidence for overlapping binding sites for the VDCC β subunit and for G$\beta\gamma$ dimers on the intracellular I-II loop (De Waard et al., 1997) and on the C and N termini (Walker et al., 1998, 1999; Canti et al., 1999) of various VDCC α1 subunits. This led to the idea that there is competition between VDCC β and G$\beta\gamma$ for the same binding site. The competition hypothesis is supported by data showing reduced G protein-mediated inhibition with overexpression of certain VDCC β subunits for several types of heterologously expressed VDCCs in *Xenopus* oocytes (Roche et al., 1995; Bourinet et al., 1996). Furthermore, previous work from our laboratory shows that partial

Received for publication 5 November 1999 and in final form 9 May 2000.
Address reprint requests to Dr. Alon Meir, Department of Pharmacology, University College London, Gower St., London WC1E 6BT, UK. Tel.: +44-20-7769-4485; Fax: +44-20-7813-2808; E-mail a.meir@ucl.ac.uk.

0006-3495/00/08/731/16 $2.00

depletion of endogenous VDCC β subunits, by an antisense oligonucleotide, enhanced inhibition of native VDCCs in sensory neurons by $GABA_B$ receptor activation, although not that by GTP-γ-s (Campbell et al., 1995b). However, facilitation or depolarization-induced relief of inhibition of N-type channels expressed in *Xenopus* oocytes was enhanced by coexpression of the VDCC β3 subunit (Roche and Treistman, 1998b), despite the reduced inhibition induced by this subunit. In addition, most descriptions of an antagonism between VDCC β and G$\beta\gamma$ dimers are based on isopotential measurements, ignoring voltage shifts related to the separate expression of VDCC β subunit or G$\beta\gamma$ with the α1 subunit. Our recent data for *Xenopus* oocytes suggest that almost all of the apparent β subunit-related antagonism of α1B modulation is due to β subunit-mediated hyperpolarization of the voltage dependence of current activation (C. Canti, Y. Bogdanov, and A. C. Dolphin, manuscript submitted for publication).

To examine the correlation between inhibition, kinetic slowing, and facilitation, we have applied several different approaches to examine the effect of VDCC β subunits on the modulation of α1B channels by G proteins in the mammalian cell line COS-7. First, we recorded single-channel α1B or α1B/β currents in two groups of cells. The first group was transfected with VDCC subunits and a minigene derived from the C terminus of a β-adrenergic receptor kinase (βARK1) (Koch et al., 1993; Stephens et al., 1998) that binds G$\beta\gamma$ and prevents basal modulation of the channels by endogenous free G$\beta\gamma$. In the second group, we transfected VDCC subunits and Gβ1γ2 dimers to produce tonic modulation. In a second approach, we recorded whole-cell currents from cells transfected with either α1B alone or α1B/β2a and the dopamine D-2 receptor to allow reversible agonist activation of endogenous G proteins. These experiments are not possible in *Xenopus* oocytes because of their endogenous VDCC β subunit (Tareilus et al., 1997).

We show that both the pronounced G$\beta\gamma$-dependent kinetic slowing of the channel response and the accompanying voltage-dependent facilitation depend on VDCC β subunit coexpression. In the absence of an expressed VDCC β subunit, Gβ1γ2 expressed tonically does not produce significant kinetic slowing of the activation of the α1B channels, while coexpression of α1B with β2a (or β1b) restores full G$\beta\gamma$ modulation. Furthermore, in the COS-7 cell expression system, transient elevation of G$\beta\gamma$ by dopamine D-2 receptor activation induces less inhibition of α1B than of α1B/β2a channels, and this is not accompanied by kinetic slowing or facilitation.

Our present findings support interdependence between the two modulatory processes induced by G$\beta\gamma$ dimers and by VDCC β subunits and may be interpreted in several ways. Either the VDCC β subunit is functionally required for the G$\beta\gamma$-induced voltage-dependent inhibition of α1B channels, or G$\beta\gamma$ is bound more strongly to the α1B subunit in the absence of a bound auxiliary β subunit. Therefore, it would unbind less easily with a depolarizing prepulse, leading to a failure to detect facilitation. The implications of both models will be discussed.

MATERIALS AND METHODS

Materials

The α1B, β1, β2a, β3, α2-δ1, βARK1 G$\beta\gamma$ binding domain minigene, D-2 receptor, and Gβ1 and Gγ2 cDNAs used in this study have been described previously (Page et al., 1997, 1998; Stephens et al., 1998; Bogdanov et al., 2000).

Transfection of COS-7 cells

COS-7 cells were cultured and transfected, using the electroporation technique, essentially as described previously (Campbell et al., 1995a; Stephens et al., 1998).

Reverse transcriptase-polymerase chain reaction

Total RNA was isolated from a pellet of COS-7 cells with an RNeasy miniprep kit (Qiagen, Crawley, UK). Residual genomic and plasmid DNA were removed by digestion with RQ DNase (Promega, Madison, WI) for 30 min at 37°C, in the presence of 40 mM Tris-HCl (pH 8.0), 10 mM $MgSO_4$, 1 mM $CaCl_2$, 40 units RNasin (Promega), and 5 units RQ DNase. Reverse transcription was carried out in a final volume of 50 μl, in the presence of 50 mM Tris-HCl (pH 8.3), 75 mM KCl, 3 mM $MgCl_2$, 10 mM dithiothreitol, 1.25 mM each deoxyribonucleoside triphosphate, 1.25 μg random hexamer primers (Promega), 40 units RNasin, and 500 units Moloney murine leukemia virus reverse transcriptase (Promega) (37°C, 60–120 min). The samples were diluted to 100 μl, and 5 μl was used per polymerase chain reaction (PCR) reaction. PCR was carried out using 1.25 units *Taq* DNA polymerase (Promega) in 25 μl, containing 10 mM Tris-HCl (pH 9), 50 mM KCl, 0.1% Triton X-100, 1.5 mM $MgCl_2$, 200 μM each of deoxyribonucleoside triphosphates, and 0.4 μM primers. The following primers were used: β1bF: CCT ATG ACG TGG TGC CTT CC; β1bR: TGC GGT TCA GCA GCG GAT TG; β2F: AAG AAG ACA GAG CAC ACT CC, β2R ACT CTG AAC TTC CGC TAA GC; β3F: CTC TAG CCA AGC AGA AGC AA; β3R: CTG GTA CAG GTC CTG GTA GG; β4F: TGA GGT AAC AGA CAT GAT GCA G; β4R: CCA CCA GTT GAA CAT TCA AGT G.

Immunocytochemistry

COS-7 cells were fixed 48 h after transfection. Cells were washed twice in Tris-buffered saline (TBS) (154 mM NaCl, 20 mM Tris, pH 7.4) then fixed in 4% paraformaldehyde in TBS as described (Brice et al., 1997). The cells were permeabilized in 0.02% Triton X-100 in TBS and incubated with blocking solution (20% (v/v) goat serum, 4% (w/v) bovine serum albumin (BSA), 0.1% (w/v) D,L-lysine in TBS). Cells were incubated for 14 h at 4°C with the appropriate primary antibody diluted in 10% goat serum, 2% BSA, 0.05% D,L-lysine. The VDCC antibodies used in this study were either raised in rabbits against specific peptides derived from a sequence common to all β subunits (β_{common}) (Campbell et al., 1995a), used at 1:500 dilution, or were produced as monoclonal antibodies to fusion proteins derived from the C-terminal sequences of β1b or β3, used at 5 $\mu g \cdot ml^{-1}$. The β1b and β3 fusion proteins consisted of amino acids 453–646 of human β1b and 403–525 of human β3. The β1b and β3 antibodies recognize the rat and human orthologs and are therefore likely to recognize the African green monkey β subunits. These specific antibodies do not cross-react with other β subunits (Day et al., 1998). The primary polyclonal antibody was detected using biotin-conjugated goat anti-rabbit IgG (0.5 $\mu g \cdot ml^{-1}$) (Sigma), then streptavidin fluorescein isothiocyanate (15 $\mu g \cdot ml^{-1}$; Molecular

Probes, Eugene, OR). For the primary monoclonal antibodies, detection was carried out with goat anti-mouse fluorescein isothiocyanate (10 $\mu g \cdot ml^{-1}$; Molecular Probes). COS-7 cells were then incubated for 20 min with the double-stranded DNA dye YO-YO (2.4 nM; Molecular Probes) to visualize the nucleus. Cells were then washed in TBS for 5 × 5 min. Coverslips were mounted directly on a microscope slide with Vectashield (Vector Laboratories, Burlingame, CA). Cells were examined on a laser-scanning confocal microscope (Leica TCS SP, Milton Keynes, UK), using conditions of constant aperture and gain, ensuring that the image was not saturated. The optical sections shown are 1 μm horizontally through the center of the cell.

Whole-cell recording

Recordings were made as described previously (Stephens et al., 1997). The internal (pipette) and external solutions and recording techniques were similar to those previously described (Campbell et al., 1995b). The patch pipette solution contained (in mM) 140 Cs-aspartate, 5 EGTA, 2 $MgCl_2$, 0.1 $CaCl_2$, 2 K_2ATP, 10 HEPES (pH 7.2), and 310 mOsm sucrose. The external solution contained (in mM) 160 tetraethylammonium (TEA) bromide, 3 KCl, 1.0 $NaHCO_3$, 1.0 $MgCl_2$, 10 HEPES, 4 glucose, 1 or 10 $BaCl_2$ (pH 7.4), and 320 mOsm sucrose. Pipettes of resistance 2–4 MΩ were used. An Axopatch 1D or Axon 200A amplifier (Axon Instruments, Foster City, CA) was used, and data were filtered at 1–2 kHz and digitized at 5–10 kHz. Analysis was performed using Pclamp6 and Origin 5. Current records after leak and residual capacitance current subtraction (P/4 or P/8 protocol) are shown. *I-V* relations were fitted with a combined Boltzmann and linear fit (because of the rectification of the channel amplitude near its reversal potential the current should be fitted with the Goldman–Hodgkin–Katz equation, but because we examined mainly the activation phase of the *I-V* relations, we used the linear approximation instead):

$$G_{max} \cdot (V - V_{rev})/(1 + e^{-(V - V_{1/2})/k}) \quad (1)$$

Voltages were not corrected for liquid junction potential (Neher, 1995), which was measured to be 6 mV in the 1 and 10 mM Ba^{2+} solutions.

Single-channel recording

All recordings were performed on green fluorescent protein (GFP)-positive cells at room temperature (20–22°C). Recording pipettes were pulled from borosilicate tubes (World Precision Instruments, Sarasota, FL) coated with Sylgard (Sylgard 184; Dow Corning, Wiesbaden, Germany) and fire polished to create high resistance pipettes (~10 MΩ with 100 mM $BaCl_2$). The bath solution, designed to zero the resting membrane potential (Meir and Dolphin, 1998) was composed of (in mM) 135 K-aspartate, 1 $MgCl_2$, 5 EGTA, and 10 HEPES (titrated with KOH, pH 7.3), and the patch pipettes were filled with a solution of the following composition (in mM): 100 $BaCl_2$, 10 TEA-Cl, 10 HEPES, 200 nM tetrodotoxin, titrated with TEA-OH to pH 7.4. Both solutions were adjusted to an osmolarity of 320 mOsmol with sucrose. Data were sampled (Axopatch 200B and Digidata 1200 interface; Axon Instruments) at 10 kHz and filtered on-line at 1 kHz. Voltages were not corrected for liquid junction potential (Neher, 1995), which was measured to be −15 mV in these solutions, so that the results could be compared with other published material. Although the junction potentials are comparable in all of the solutions used here, the activation curves are shifted to more depolarized potentials with increased Ba^{2+} concentration. This is likely to be due to surface charge effects caused by the elevated Ba^{2+}. The $V_{1/2}$ values for the *I-V* curves (for α1B/β2a/G$\beta\gamma$ or α1B/β2a/D-2+quinpirole) were +3.5mV with 1 mM (Fig. 1 *b*), +24.8 mV with 10 mM (Fig. 6 *e*), and +43.5mV with 100 mM Ba^{2+} (a fit with Eq. 1 to the data shown in Fig. 3 *f*, defining V_{rev} as the extrapolated V_{rev} from the linear regression fitted to the single-channel amplitudes).

Single-channel analysis

Leak subtraction was performed by averaging segments of traces with no activity from the same voltage protocol in the same experiment and subtracting this average from each episode, using pClamp6. Event detection was carried out using the half-amplitude threshold method. Single-channel amplitude was determined, either by a Gaussian fit to the binned amplitude distributions, or by the mean amplitude in cases when there was a small number of events or multiple conductance modes (see Fig. 2 *c*). However, the values obtained here (13pS) are smaller than those reported elsewhere (see, for example, Carabelli et al., 1996) and by us (Meir and Dolphin, 1998). This may be due to the inclusion of the low-amplitude events in the present study (see below). The open time was determined as the arithmetic mean of the binned open times. In this way the events shorter than 0.1 ms are ignored, and the resulting value is higher than the one given by an exponential fit to the open time distributions.

As reported previously (Meir and Dolphin, 1998), HVA VDCCs also show a lower amplitude mode, which may represent a subconductance state. Here the low-amplitude events were included in the ensemble current and cumulative first latency (CFL) analysis. The low-amplitude events represent, on average, between all subunit compositions ($n = 9$, single channel patches), 25.1 ± 3.7% of the openings, and in this study we did not examine their particular contribution to the processes tested. No patches were included in this study that only showed low-amplitude events, as reported previously (Meir and Dolphin, 1998). For mean open time measurements, we did not include the low-amplitude events. Latency to first opening was measured in 2-ms bins and, if necessary, was corrected for the number of channels in the patch (see below).

Estimation of the number of channels in the patch

We assumed the number of detectable multiple openings to represent the number of channels active in the patch. This assumption is supported by confirmation that in patches where no multiple openings were detected, there is a high probability that it results from only a single channel present. For all of the single detected channel patches, we calculated the number of expected double openings if there were two channels in the patch. The number of double openings expected was calculated from

$$n_{oo} = N \cdot (\text{mean open time})/(2 \cdot (\text{mean closed time})) \quad (2)$$

n_{oo} is the expected number of double openings, and N is the number of single openings (Colquhoun and Hawkes, 1995). n_{oo}/N gives the proportion of double opening events expected for α1B/βARK1 (12.3 ± 5.5%, $n = 3$), α1B/G$\beta\gamma$ (5.7 ± 2.7%, $n = 3$), α1B/β2a/βARK1 (46.5 ± 13.5%, $n = 2$), and α1B/β2a/G$\beta\gamma$ (29.3 ± 5.6%, $n = 4$), all at +30 mV. In all of these patches, no double openings were detected at any voltage examined. The mean number of estimated channels was similar for all subunit compositions. Here it is given with the distribution of the number of channels, for each subunit composition: α1B/βARK1 (2.8 ± 0.3, $n = 13$; two patches with one channel, three with two, three with three, and five with four), α1B/G$\beta\gamma$ (2.7 ± 0.4, $n = 13$; three patches with one channel, three with two, five with three, one with four, and one with seven), α1B/β2a/βARK1 (2.5 ± 0.4, $n = 11$; two patches with one channel, four with two, four with three, and one with five), and α1B/β2a/G$\beta\gamma$ (2.2 ± 0.3, $n = 14$; five patches with one channel, four with two, three with three, one with four, and one with five). This method provides an underestimate of the number of channels.

Latency analysis and correction for multichannel patches

First latency histograms from each experiment were divided by the number of episodes collected, to express the data as a probability (Imredy and Yue,

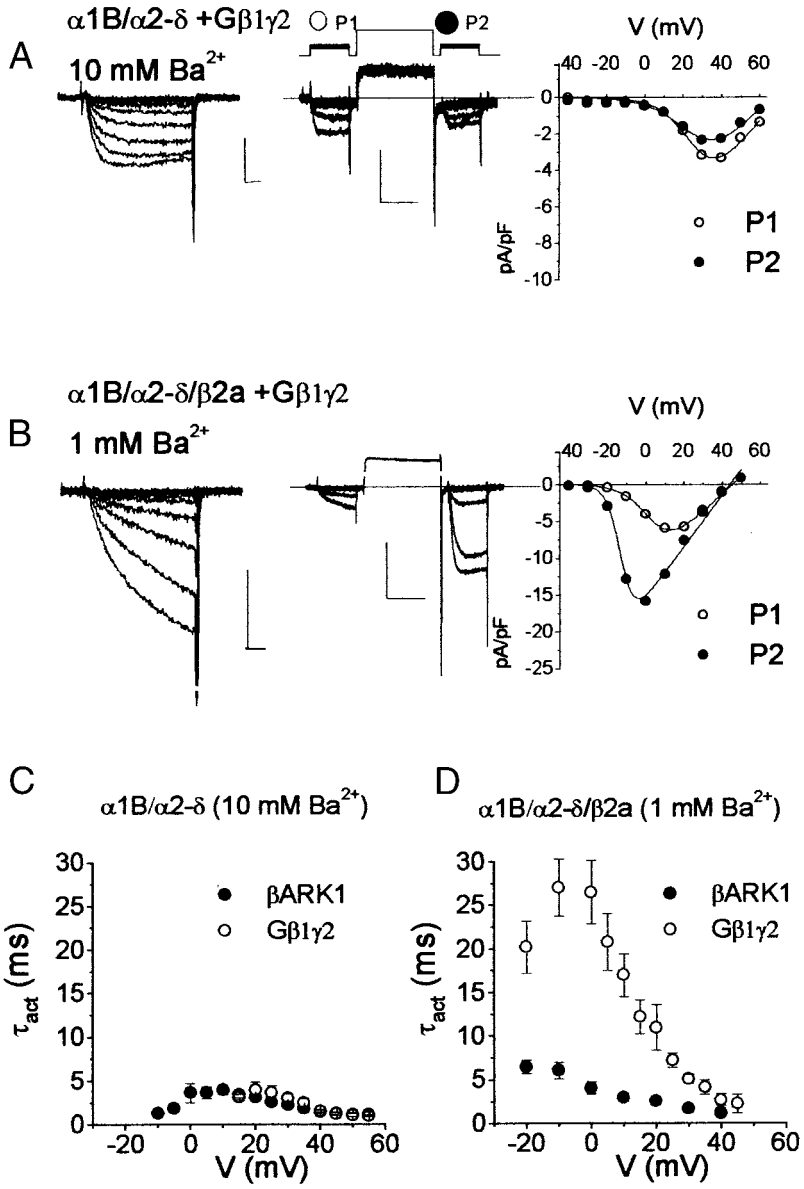

FIGURE 1 Tonic inhibition of N-type channels, coexpressed with G$\beta1\gamma2$ in COS-7 cells. (*a*) α1B/α2-δ/G$\beta\gamma$ channels, with 10 mM Ba^{2+} as charge carrier. *Left*: Current responses to 50-ms test pulses to −10 to +35 mV, in 5-mV intervals. The scale bars represent 5 pA/pF and 10 ms. *Middle*: A typical response to the double pulse protocol (holding potential = −80 mV, test potentials from −10 mV to 30 mV in 10-mV intervals). The scale bars represent 10 pA/pF and 50 ms. *Right*: *I-V* relationship (taken at the peak current) for the experiment shown in the middle panel, fitted with a combined Boltzmann and linear fit (see Materials and Methods). $V_{1/2}$ was +26.6 mV and +26.8 mV for P1 and P2, respectively, and the *k* factor was 7.9 mV and 9.7 mV for P1 and P2, respectively. (*b*) α1B/α2-δ/β2a/G$\beta\gamma$ channels with 1 mM Ba^{2+} as charge carrier. *Left*: Current responses to 50-ms test pulses to −35 to +10 mV, in 5-mV intervals. The scale bars represent 20 pA/pF and 10 ms. *Middle*: A typical response to double pulse protocol (holding potential = −80 mV, test potentials from −40 mV to 0 mV in 10-mV intervals). The scale bars represent 10 pA/pF and 50 ms. *Right*: *I-V* relationship (taken at 50 ms) for the experiment shown in the middle panel, fitted with a combined Boltzmann and linear fit (see Materials and Methods). $V_{1/2}$ was +3.5 mV and −13.0 mV for P1 and P2, respectively, and the *k* factors were 6.8 mV and 3.6 mV for P1 and P2, respectively. (*c*) Comparison of the activation time constants (τ_{act}) for α1B/α2-δ channels cotransfected with βARK1 (*n* = 12, ●) or with G$\beta\gamma$ (*n* = 5, ○). The activation phase of currents was fitted with single exponential at all voltages. (*d*) Comparison of the activation time constants for α1B/α2-δ/β2a channels cotransfected with βARK1 (*n* = 5, ●) or with G$\beta\gamma$ (*n* = 10, ○).

1994). The plots were then accumulated, using an Origin built-in function, according to

$$CFL_N = \Sigma(FL_N)/E \quad (3)$$

FL_N and CFL_N are the first latency and the cumulative first latency distributions, respectively, and *E* is the number of stimulations. Multichannel patches were also corrected for the apparent number of channels in the patch, according to

$$CFL_1 = 1 - (1 - CFL_N)^{(1/N)} \quad (4)$$

CFL_1 and CFL_N are the single-channel and multichannel cumulative first latency functions, respectively, and *N* is the apparent number of channels.

Data are expressed as mean ± SEM. Statistical analysis was performed using a paired or unpaired Student's *t*-test or two-way analysis of variance (ANOVA), as appropriate.

RESULTS

Tonic inhibition of α1B channels by G$\beta\gamma$ cotransfection in COS-7 cells

A detailed analysis of the activation pattern of the currents formed by α1B compared to the α1B/β combination was obtained by driving the free G$\beta\gamma$ concentration to extremes; we either achieved tonically elevated G$\beta\gamma$ levels by cotransfection of G$\beta1\gamma2$, or minimized endogenous G$\beta\gamma$ with βARK1 minigene cotransfection. The VDCC β2a subunit was used in this study to remove confounding effects of inactivation so that activation could be examined in isolation. In the whole-cell experiments, α2-δ was also included in the transfections, but similar results were obtained with-

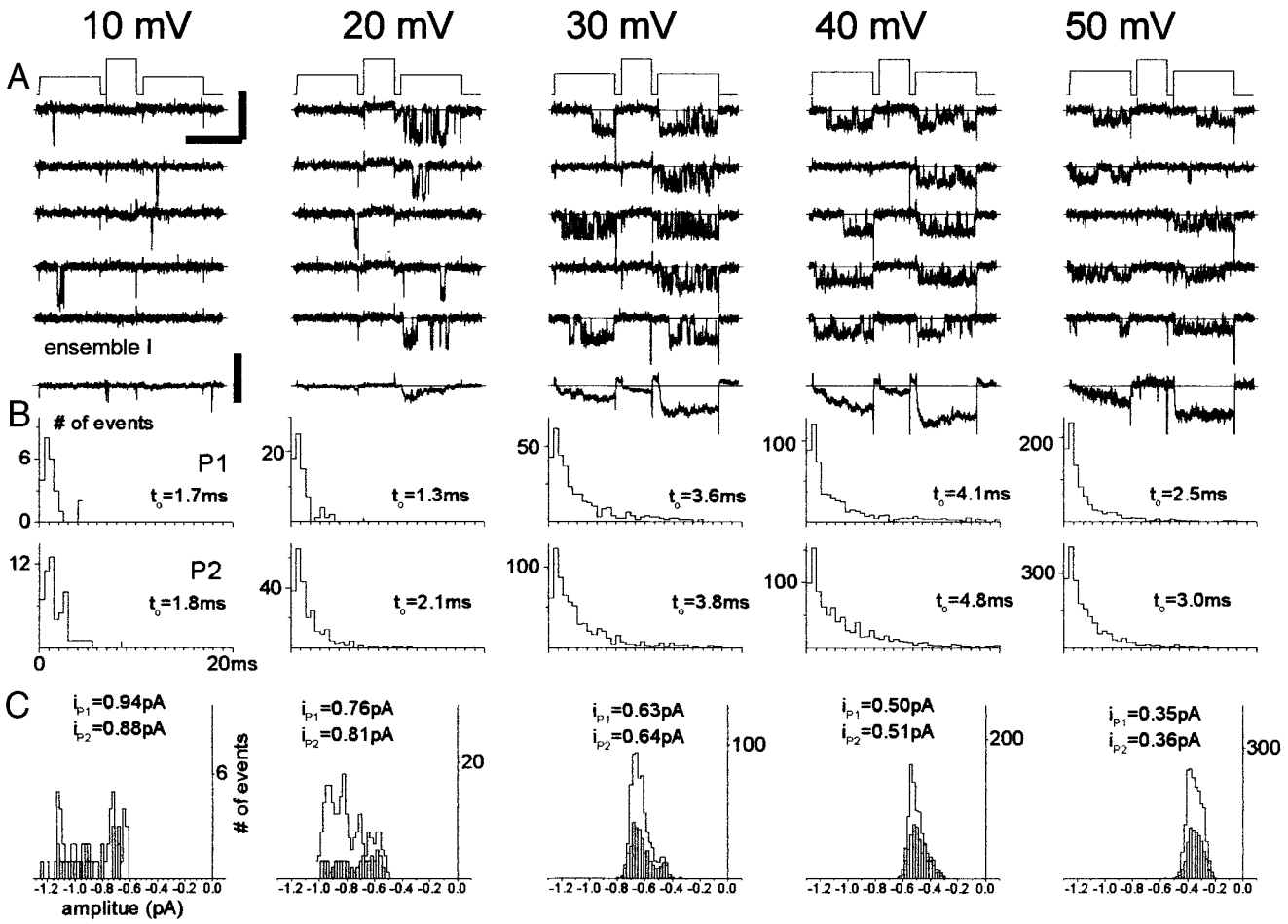

FIGURE 2 Examples of single-channel activity and its analysis, for α1B in combination with β2a in the presence of G$\beta\gamma$2. (*a*) *Top voltage trace*: Holding potential −100 mV, test potential in both P1 and P2, to the indicated value, 100 ms, separated by a strong depolarizing prepulse (+120 mV, 50 ms). Steps were delivered every 2 s. The voltage protocol is followed by five representative traces and an ensemble of 200 episodes (*bottom trace*) for each voltage. The zero current line that runs through the traces represents the closed state; openings are downward deflections. The bars to the right of the first trace represent 1 pA and 100 ms, and the bar to the right of the ensemble current trace represents 0.2 pA (this applies to all of the voltages). (*b*) Open time distribution histograms corresponding to the experiment shown in *a* for P1 (*top histogram*) and P2 (*bottom histogram*). For each voltage 200 episodes were collected. The bin width was 0.5 ms. The mean open time at each voltage is indicated. (*c*) Open level amplitude histograms for the different voltages in P1 (*bars*) and P2 (*line*). The bin width was 0.02 pA. The mean amplitude is indicated for P1 and P2.

out the additional inclusion of this subunit (data not shown, but see the single-channel results).

α1B/α2-δ/G$\beta\gamma$2 whole-cell currents were rapidly activating (Fig. 1 *a*, *left*) and showed no facilitation in response to a prepulse to +120 mV, but rather showed some inactivation (Fig. 1 *a*, *middle*). The *I-V* relation parameters did not change with a depolarizing prepulse, indicating the lack of facilitation (Fig. 1 *a*, *right*). In sharp contrast, with β2a coexpression (Fig. 1 *b*), the α1B/α2-δ/β2a/G$\beta\gamma$2 currents activated slowly (Fig. 1 *b*, *left*) and were strongly facilitated by a large depolarizing prepulse (Fig. 1 *b*, *middle* and *right*). The prepulse produced a −16-mV hyperpolarizing shift in the *I-V* relation and increased the current amplitude (Fig. 1 *b*, *right*).

The speed of the activation process and its voltage dependence were estimated by fitting a single exponential to the activation phase of the whole-cell current. Comparison of activation time constants (τ_{act}) obtained for α1B/α2-δ channels, cotransfected with βARK1 or G$\beta\gamma$2, showed no significant differences (Fig. 1 *c*). Nevertheless, a slight depolarizing shift in the τ_{act}-voltage relation was evident with G$\beta\gamma$2 (compare *empty* to *filled circles* in Fig. 1 *c*). In contrast, with the additional coexpression of β2a (Fig. 1 *d*), τ_{act} was about fivefold slower with G$\beta\gamma$2 compared to βARK1 cotransfection.

Single-channel analysis of tonic inhibition of α1B channels by G$\beta\gamma$

We analyzed single-channel records over a wide range of voltages (Fig. 2 *a*) and compared a number of parameters,

including single-channel ensemble current (Fig. 2 *a*), mean open time (Fig. 2 *b*), mean amplitude (Fig. 2 *c*), and latency to first opening. The behavior of single channels recorded from cell-attached patches of COS-7 cells transfected with α1B with or without a VDCC auxiliary β subunit and either G$\beta\gamma$ or βARK1 (Fig. 3 and 4) was compared using these parameters.

These parameters enable one to distinguish between the effects of either modulatory protein (G$\beta\gamma$ and/or VDCC β) on activation (all of the processes leading to the first opening of a channel) or postactivation processes, including mean open time. The hypothesis suggested by the whole-cell data is that the related voltage-dependent processes of kinetic slowing and prepulse facilitation, which are both thought to involve G$\beta\gamma$ unbinding (Stephens et al., 1998; Zamponi and Snutch, 1998), are dependent on the presence of the VDCC β subunit. We also examined whether parameters independent of the activation process, such as amplitude and mean open time, are affected by either modulatory protein.

Both the mean open time and mean amplitude represent compound processes (see Fig. 2 *c* for the compound amplitude distributions). The open time distribution of expressed (Wakamori et al., 1999) N-type channels was described by the sum of several exponentials. However, because of the exclusion of the shortest open times in our analysis, the contribution of the shorter exponent could be misinterpreted. We therefore chose to examine the arithmetic mean open time (Fig. 2 *b*). Changes in this parameter could therefore be a result of either a change in the distribution between short and long opening populations or in the time constants for channel closure.

Cells expressing α1B/βARK1 (Fig. 3 *a, left*) showed channels with a single-channel conductance of 13 pS and a reversal potential of +71 mV (Fig. 3 *b, filled triangles*). The channels had a mean open time at +20 mV of 1.7 $\pm$ 0.1 ms ($n = 7$; Fig. 3 *b, top*) and showed a tendency to inactivate during the test pulse (see *traces* in Fig. 3 *a, left*). All of the patches were subjected to double pulse protocols, with a second test step after a 50-ms prepulse to +120 mV (Fig. 3 *a, top trace*). The ensemble average current at +30 mV showed no significant difference in the mean responses to the same voltage step in P1 and P2 (Fig. 3 *a, left, bottom trace*). This was true for all of the voltages examined (Fig. 3 *b, middle*, compare *filled circles* and *squares*).

Coexpression of the VDCC α1B subunit with Gβ1γ2 (Fig. 3 *a, right*) yielded channels with very similar single-channel conductance and reversal potential (Fig. 3 *b, empty triangles*). The mean open time was shorter over the voltage range examined ($p < 0.001$ between the α1B/βARK and α1B/G$\beta\gamma$ populations; two-way ANOVA). For example, at +20 mV the mean open time was 1.1 $\pm$ 0.1 ms ($n = 9$), which is a 35% reduction compared to that obtained for α1B/βARK ($p < 0.05$, Student *t*-test; Fig. 3 *b, top*). In agreement with the whole-cell data (Fig. 1 *a*), the responses to P1 and P2 were similar within the voltage range examined (Fig. 3, *a* and *b*), indicating a lack of facilitation. There were no significant differences between these two groups of data. Nevertheless, a small ~5-mV depolarizing shift of the single-channel *I-V* relationship (Fig. 3 *b, middle*) was detected in the presence of Gβ1γ2, which was similar to the shifts observed in whole-cell recordings.

The coexpression of VDCC β2a with α1B markedly affected the activity of the resulting channels (Fig. 3 *c*). However, the single-channel conductance was unchanged (Fig. 3 *d*). The mean open time was increased significantly by VDCC β subunit expression at all of the voltages examined (Student's *t*-test, $p < 0.05$ for all six pairs of data) (compare Fig. 3 *b, top*, and Fig. 3 *d, top*). However, the mean open time was similar regardless of the presence or absence of G$\beta\gamma$ (Fig. 3 *d, top*). The α1B/β2a/βARK1 channels showed fast activation and no inactivation (Fig. 3 *c, left*). The double pulse protocol did not reveal significant differences in the responses to P1 and P2, but slight facilitation was evident at most voltages (Fig. 3 *c, left*, and Fig. 3 *d, filled symbols*). This is in agreement with whole-cell recordings showing that coexpression of VDCCs with βARK1 removed most but not all of the facilitation (Stephens et al., 1998). The ensemble average currents of these channels were about twofold larger in amplitude than in the absence of coexpressed β2a (compare *filled squares* in Fig. 3, *b* and *d*).

Transfection of Gβ1γ2 instead of βARK1 with α1B/β2a yielded channels with a similar mean open time and single-channel conductance (Fig. 3, *c, right*, and *d, empty symbols*). However, α1B/β2a/Gβ1γ2 channels frequently failed to gate to the open state during the 100-ms test pulse, giving rise to a large proportion of null episodes. If the channel opened, it was usually with a long delay (Fig. 3 *c, right*). Under this condition, the double pulse protocol was very effective at eliciting facilitation of both the ensemble current amplitude (Fig. 3 *c, right, bottom trace*, and Fig. 3 *d*, compare *empty symbols*) and the kinetics of the response. Superimposing the responses to a +40-mV test pulse (P1) for α1B/Gβ1γ2 and α1B/β2a/Gβ1γ2 shows clearly that in the additional presence of β2a the mean single-channel response of α1B/Gβ1γ2 developed much more slowly (Fig. 3 *e*).

Influence of VDCC β2a on G$\beta\gamma$ modulation of latency to the first opening

Single-channel studies that have analyzed the effect of neurotransmitter-activated G protein modulation of N-type channels (Carabelli et al., 1996; Patil et al., 1996) suggest that the main parameter change is a slowing in the activation process, manifested by a longer latency to first opening. Therefore we compared the first latency, presented in the form of CFL (see Materials and Methods), for the different combinations of expressed subunits. CFL represents the

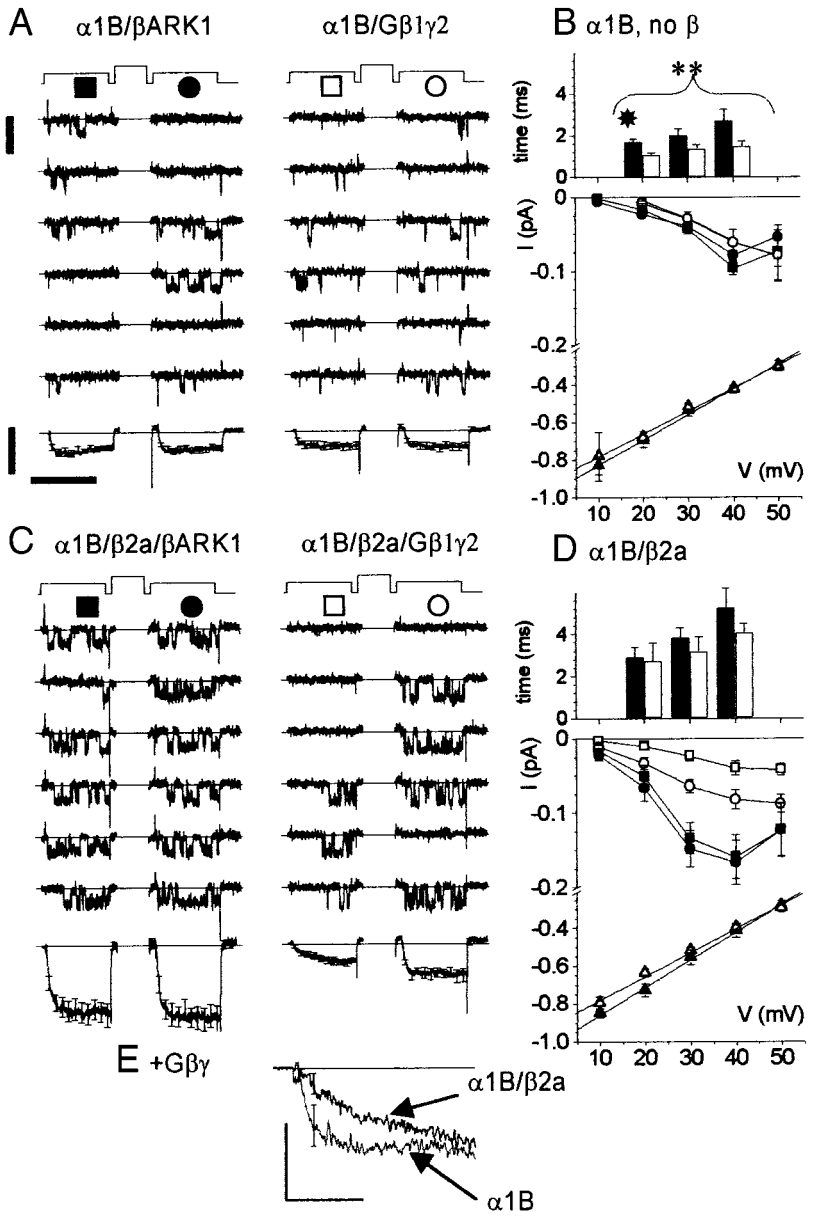

FIGURE 3 Single-channel activity of α1B in combination with βARK1 or G$\beta1\gamma2$ in the presence or absence of β2a. (*a*) *Top voltage trace*: Test potential in both P1 and P2, +30 mV, separated by a depolarizing prepulse to +120 mV. *Left column*: The single-channel records represent a single-channel patch with α1B/βARK1. The bar to the left of the first trace represents 1 pA (this applies to all of the single-channel traces). *Bottom trace*: Average ± SEM (errors shown only every 5 ms for clarity), single-channel ensemble current (see Materials and Methods) at +30 mV (n = 13, 1895 episodes included). The bars apply to all of the ensemble traces in *a* and *c* and represent 0.1 pA and 100 ms. In all panels, the interpulse response was clipped for clarity. *Right column*: A representative, apparently single-channel patch with α1B/G$\beta1\gamma2$. The format is the same as in *a*. *Bottom trace*: n = 13, 2640 episodes included. (*b*) *Top*: Mean channel open time for data of the type shown in *a*, α1B/βARK1 (*filled columns*, n = 7) and α1B/G$\beta\gamma$ (*empty columns*, n = 9). Statistical significance is $p < 0.05$ (Student's t-test, noted by * for a single voltage level) and $p > 0.001$ (two-way ANOVA, noted with bracket and **) for the difference between the two populations. *Bottom*: Current-voltage relationship for ensemble and unitary currents (note the break in scale). α1B/βARK1: P1 ■ and P2 ●; α1B/G$\beta\gamma$: P1 □ and P2 ○. Single-channel ensemble current amplitudes were taken as the current at 20 ms (the average of 19–21 ms) after the onset of the test pulse (mean ± SEM). Unitary amplitudes were fit with a linear regression. The single-channel conductance was 13 pS and 12 pS, and the reversal potential was +70.9 mV and 73.8 mV for α1B/βARK1 (▲) and α1B/G$\beta\gamma$ (△), respectively. (*c*) Representative single-channel patches with α1B/β2a. *Left column*: α1B/β2a/βARK1, the same format as in *a*. *Bottom trace*: n = 13, 1460 episodes included. *Right column*: α1B/β2a/G$\beta\gamma$. *Bottom trace*: n = 12, 3120 episodes included. (*d*) *Top*: Mean channel open time for data of the type shown in *c*, α1B/β2a/βARK1 (*filled column*, n = 5) and α1B/β2a/G$\beta\gamma$ (*empty column*, n = 5). *Bottom*: *I-V* curves for α1B/β2a channels. The same format as in *b*, α1B/β2a/βARK1: P1 ■] and P2 ●; α1B/β2a/G$\beta\gamma$: P1 □ and P2 ○. The single-channel conductance was 14 pS and 12 pS, and the reversal potential was +68.7 mV and +71.8 mV for α1B/β2a/βARK1 (▲) and α1B/β2a/G$\beta\gamma$ (△), respectively. (*e*) The activation phases at +40 mV of the ensemble average responses to P1 with G$\beta\gamma$ are compared for α1B (n = 13) and α1B/β2a (n = 11). The scale bars represent 0.05 pA and 20 ms.

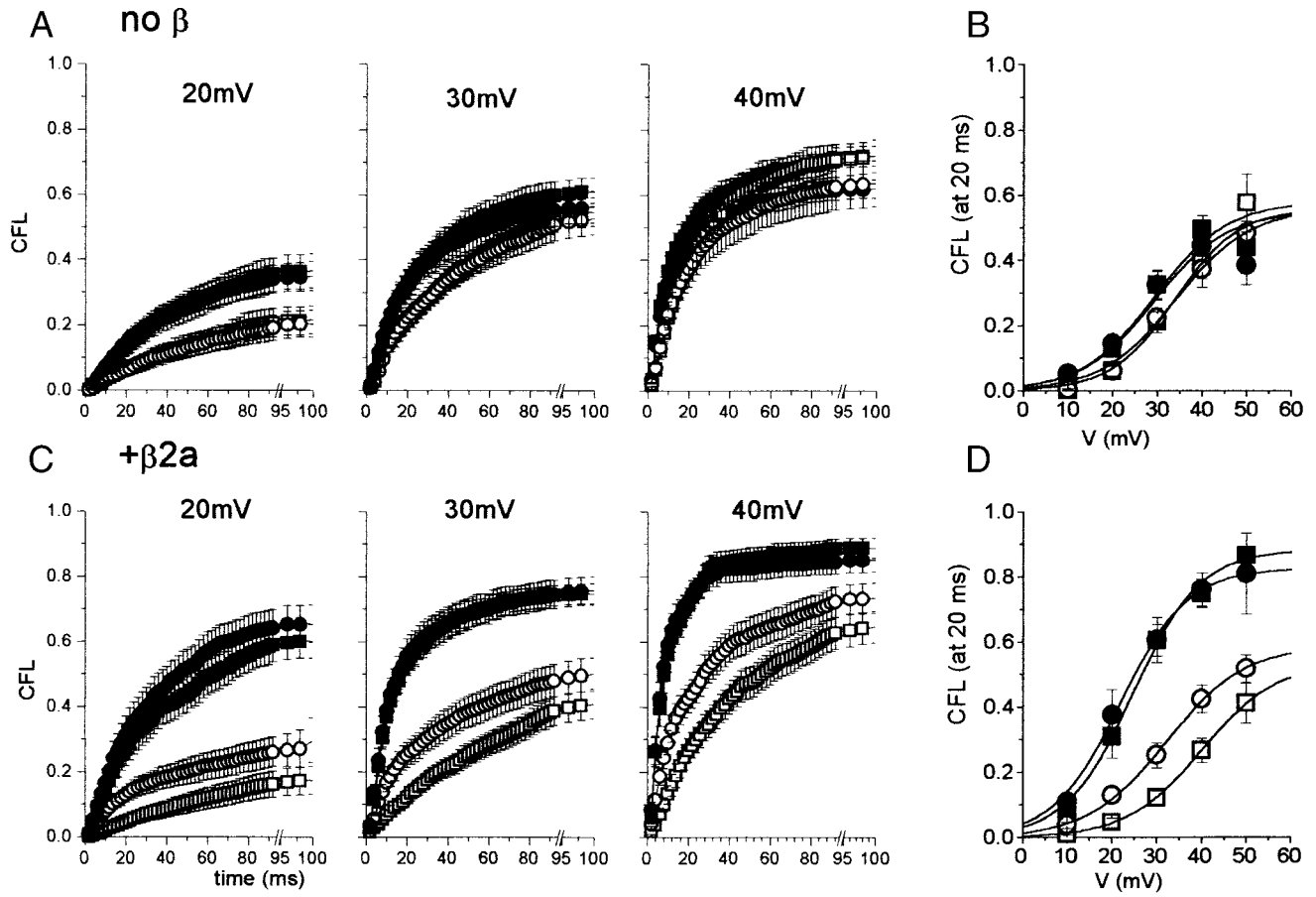

FIGURE 4 First latency of α1B/βARK1 compared to α1B/G$\beta\gamma$ and of α1B/β2a/βARK1 compared to α1B/β2a/G$\beta\gamma$. Latency to first opening was measured in single and multichannel patches (see Materials and Methods). The cumulative first latency (CFL) plots for all of the experiments with the same subunit composition were averaged, and the means ± SEM are shown. The CFL represents the probability of the channel opening before a given time (see Materials and Methods). (*a*) Opening probability (CFL) without the β subunit at three different voltages; the voltage step is indicated above each column. α1B/βARK1: P1 (■) and P2 (●); α1B/G$\beta\gamma$: P1 (□) and P2 (○). The *x* axis was broken between 94 and 95 ms to expand the last few symbols for clarity of the symbol definition. (*b*) The opening probability (CFL) 20 ms after the onset of the test pulse (the same symbol code as in *a*). Boltzmann fits to the data are plotted as continuous lines. The extracted parameters are as follows: for α1B/βARK1: P1, P2 (n = 13); for α1B/G$\beta\gamma$: P1 and P2 (n = 13), respectively. Maximum (%), 58, 55, 56, and 56. $V_{1/2}$ (mV), 29, 29, 34, 34. (*c*) Opening probability with the combinations including the β subunit at three different voltages. Symbols are as in *a*. (*d*) The opening probability 20 ms after the onset of the test pulse for α1B/β2a/βARK1 and α1B/β2a/G$\beta\gamma$ (the same symbol code as in *a*). Boltzmann fits to the data are plotted as continuous lines. The extracted parameters are as follows: for α1B/β2a/βARK1: P1, P2 (n = 13); for α1B/β2a/G$\beta\gamma$: P1 and P2 (n = 12), respectively. Maximum (%), 88, 83, 53, and 59. $V_{1/2}$ (mV), 25, 22, 40, 32.

kinetics of the opening probability of the channel, i.e., the probability that the channel will open before any given time in the test pulse. Thus higher values at a given point in time represent faster activation kinetics.

Both α1B/Gβ1γ2 and α1B/βARK1 channels showed voltage-dependent kinetics of activation that were insensitive to the large depolarizing prepulse (Fig. 4 *a*; compare the almost superimposed *square* and *circular symbols*). A Boltzmann fit to these data revealed that the activation process remained partial, reaching saturation at 50–60% (Fig. 4 *b*). This may have been due to closed-state inactivation (Patil et al., 1998). There were no significant differences between the individual CFL values 20 ms after the onset of the test pulse, but there was a +5-mV shift in the $V_{1/2}$ with Gβ1γ2 (Fig. 4 *b*).

The expression of α1B/β2a/βARK1 resulted in rapidly activating channels (Fig. 4 *c*, *filled symbols*), with a more negative midpoint of activation than in the absence of a β subunit, and maximum activation of ~85% at 20 ms (Fig. 4 *d*). On the other hand, expression of α1B/β2a/Gβ1γ2 resulted in channels that were slowly activating and therefore showed very low opening probabilities (Fig. 4 *c*, *empty squares*). Application of a strong depolarizing prepulse resulted in a biphasic activation waveform (Fig. 4 *c*, *empty circles*). The added fast component facilitated the opening probability (Fig. 4 *d*, *compare empty circles* and *empty squares*).

To examine whether the effects of β2a on facilitation (compare the P2/P1 ratio in Fig. 5, *a* and *b*) were a general feature of VDCC β subunit coexpression, we also used the

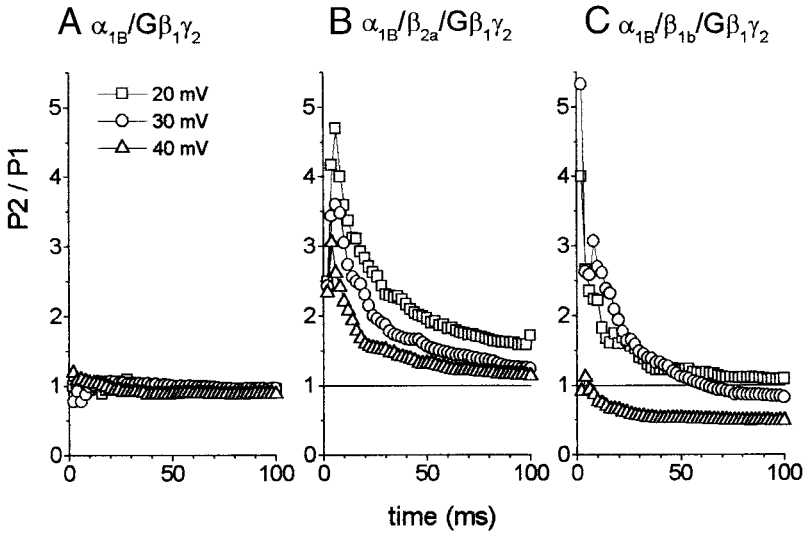

FIGURE 5 Facilitation of α1B/G$\beta\gamma$ channels coexpressed either with no VDCC β subunit or with β2a or β1b. (*a*) Lack of prepulse facilitation of α1B/G$\beta\gamma$ without expression of the VDCC β subunit. The CFL generated for the response to P2 was divided by that of P1 (P2/P1) and plotted against time. □, +20 mV; ○, +30 mV; △, +40 mV (n = 13). (*b*) Facilitation of the opening probability by a prepulse occurs in the presence of β2a. Conditions and symbols are as in *a* (n = 12). (*c*) Facilitation at low voltages and inactivation at high voltages of the opening probability by a prepulse occurs in the presence of β1b. Conditions and symbols are as in *a* (n = 10).

β1b subunit instead of β2a. Here, because α1B/β1b currents showed inactivation, the influence of a prepulse was more complex, increasing both facilitation and inactivation (Fig. 5 *c*). Thus the P2/P1 waveform showed strong facilitation at low voltages (*empty squares* in Fig. 5 *c*) and inactivation at higher voltages (Fig. 5 *c*, *empty triangles*). Interestingly, at +30 mV (Fig. 5 *c*, *empty circles*), the activation was strongly facilitated at the beginning of the voltage pulse and inactivated at its end.

Dopamine D-2 receptor-mediated inhibition of α1B channels in COS-7 cells

The differential expression of βARK1 or G$\beta\gamma$ with α1B channels did not allow direct observation of the process of inhibition of the channels by activated G$\beta\gamma$. We therefore examined the effect of receptor activation of G proteins on α1B (Fig. 6, *a–c*) or α1B/β2a (Fig. 6, *d–f*) currents. It should be noted that in these experiments, the basal G$\beta\gamma$ concentration results in partial tonic modulation of the α1B VDCCs (see the control facilitation in Fig. 6 *e*). When α1B channels, coexpressed with the dopamine D-2 receptor, were expressed without a VDCC β subunit, the mean current (at +10 mV) showed 24.5 ± 9.7% inhibition (n = 12, $p < 0.05$, for the current values before normalization) upon application of a maximum concentration (100 nM) of the D-2 agonist quinpirole (Fig. 6 *a*), but unequivocal inhibition was detected in only six of 12 cells. The mean voltage-dependent parameters for the *I-V* curves were unaffected either by quinpirole or by a depolarizing prepulse in the presence of quinpirole (Fig. 6 *c* and Table 1). This residual inhibition by quinpirole was not associated with slowed activation or with facilitation by a depolarizing prepulse (Fig. 6, *a* and *c*).

In contrast, when β2a was coexpressed with the α1B subunit, the typical features of G protein modulation were detected. Activation of the D-2 receptor with quinpirole produced stronger and much more reproducible inhibition (56.5 ± 7.8%, n = 14, $p < 0.05$, for the current values before normalization and versus no VDCC β, at +10 mV). The extent of inhibition by quinpirole was probably an underestimate in this case, because of preexisting tonic modulation in the control, which is partially removed on recovery (Fig. 6 *d*). This inhibition was associated with slowed activation (Fig. 6, *d* and *e*, and Table 1) and voltage-dependent facilitation (Fig. 6, *d–f*). The *I-V* curves showed a significant hyperpolarizing shift due to the prepulse, before quinpirole application, which was increased during agonist application. There was also a marked depolarizing shift due to quinpirole application (Fig. 6 *f* and Table 1). In α1B/β2a subunit combination, the voltage dependence of activation was very sensitive both to a prepulse and to quinpirole (see *k* factors in Table 1).

A possible reason for the heterogeneity of the effect of quinpirole in the absence of coexpressed VDCC β subunit is that endogenous VDCC β subunits may be present in some or all COS-7 cells to a varying extent. To test for endogenous VDCC β subunits, reverse transcriptase-polymerase chain reaction (RT-PCR) was carried out on mRNA isolated from COS-7 cells. As calcium channel β subunits have not been cloned from African green monkey (COS-7 cells), all available sequences from different species (human, rat, mouse, and rabbit) were aligned, and primers were designed to anneal to conserved regions. Untransfected cells showed detectable but low levels of PCR product for all four β subunits, β1b, β2a, β3, and β4, of a size identical to that observed in cells transfected with the specific subunit (Fig. 7 *a*), although it must be pointed out that PCR was carried out under saturating, and therefore nonquantitative, conditions. We tested for endogenous protein products of these transcripts by immunocytochemistry with either pan-specific β antibodies (not shown) or specific β1b and β3

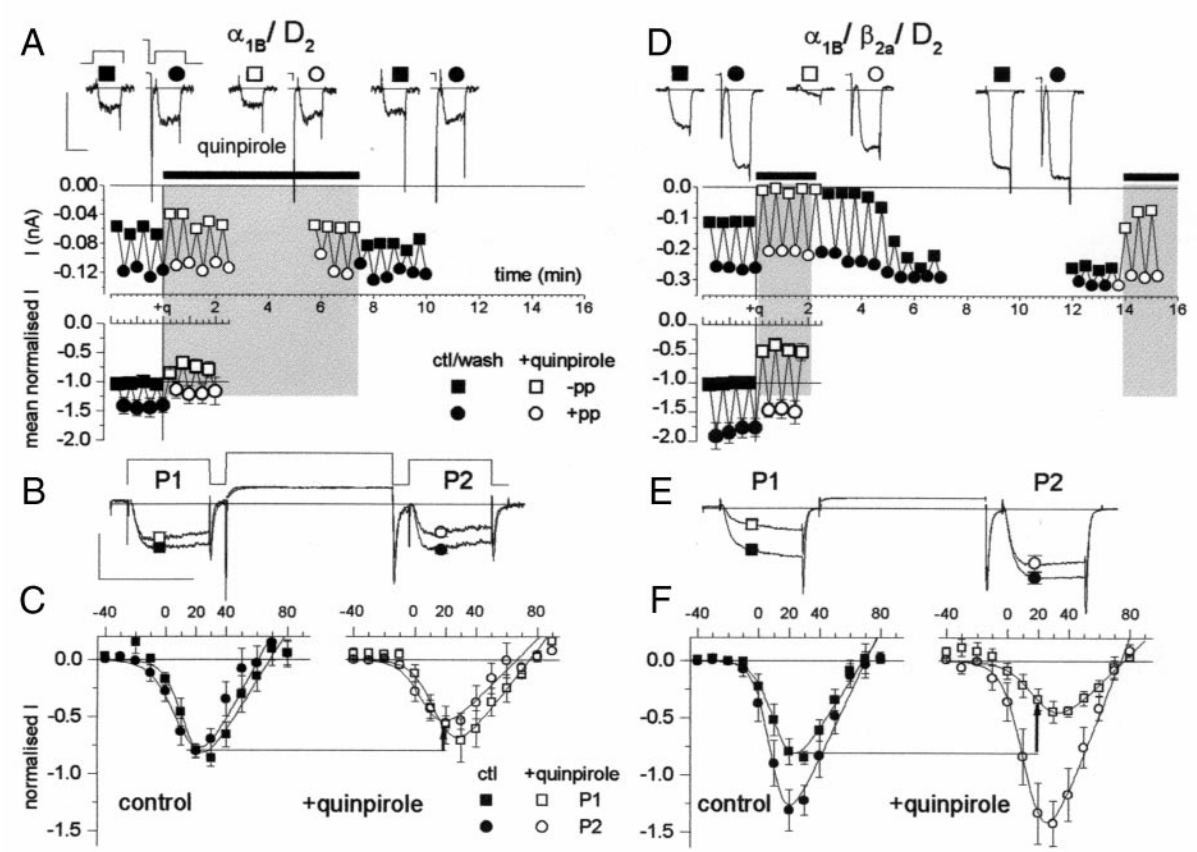

FIGURE 6 D-2 dopamine receptor-activated G protein modulation of α1B channels. Whole-cell currents recorded from COS-7 cells transfected with α1B/D-2 (*a–c*) or α1B/β2a/D-2 (*d–f*), with 10 mM Ba^{2+} as the charge carrier. (*a*) Time course for quinpirole inhibition of α1B/D2 currents. The voltage protocol consists of a single 50-ms test pulse to +10 mV, either preceded (*circles*) or not (*squares*) by the 100-ms prepulse to +120 mV, delivered alternately every 15 s. (The prepulse is clipped, for better time resolution of the test current shown. However, both a step from positive current and a tail current precedes the test pulse response, followed by a prepulse.) At the top are shown examples of responses to such a protocol, before (*left*), during (*middle*), and after (*right*) bath perfusion of 300 nM quinpirole (both during control and wash; the bath was perfused with bath solution). The bars also apply to *d* and represent 200 pA and 50 ms. A time course of this experiment is presented as the upper time course. The period of quinpirole perfusion is marked with a bar and shading (7 min in this case). The monitoring was interrupted after 2.5 min. to record an *I-V* (shown below), and the time course was then resumed to record washout of the drug. The mean normalized amplitudes of the responses, alternately with (*circles*) and without (*squares*) a prepulse, are shown in the lower time course. The mean of four pulses after the start of application of quinpirole shows that the current amplitude was smaller by 24.5 ± 9.7% (n = 12), measured 20 ms after the onset of the test pulse. In each experiment the currents were aligned to the point of the drug application and normalized to the value of the episode at position −3 (45 s before drug application) in the figure. (*b*) Mean normalized current elicited by a 50-ms test potential to +20 mV, delivered every 15 s, before (P1) and after (P2) a prepulse to +120 mV for 100 ms (holding potential, −80 mV), before (P1 ■ and P2 ●) and after (P1 □ and P2 ○) application of the D-2 agonist quinpirole. Currents were normalized to the current at 20 ms after the onset of the test pulse in P1 before quinpirole application and then averaged. The scale bars apply to *a* and *d* and represent one normalized current unit and 50 ms. Representative mean ± SEM are shown in the same symbols. (*c*) Mean normalized *I-V* curves for α1B/D2 (n = 9), before (*left*) and during (*right*) application of quinpirole. All values were normalized to the peak current in P1 before quinpirole application. The data were fit with a combined Boltzmann and linear fit (see Materials and Methods). Before drug application (*left*), $V_{1/2}$ (mV) was 15.3 ± 2.4 and 12.1 ± 2.4, and k (mV) was 5.7 ± 0.4 and 7.1 ± 0.6, in P1 and P2, respectively. During drug application (*right*) $V_{1/2}$ (mV) was 18.7 ± 2.1 and 16.0 ± 3.1, and k (mV) was 6.9 ± 0.8 and 7.8 ± 1.0, in P1 and P2, respectively. The amount of inhibition at +20 mV is indicated by the vertical arrow. (*d*) Time course for quinpirole inhibition of α1B/β2a/D2 current (format as in *a*). Examples of responses and the time course of one experiment are shown as in *a*. The monitoring was broken during the recovery phase after 7 min to record an *I-V* (not shown) and resumed to record a second drug application. This demonstrates the reversible effect of quinpirole. Mean normalized α1B/β2a/D2 current amplitude is shown on the lower trace for responses at +10-mV test pulses (n = 14, the same format as in *a*). The corresponding inhibition was 56.5 ± 7.8%. (*e*) α1B/β2a coexpressed with dopamine D-2 receptors. Voltage protocol and symbols as in *a* (n = 9). (*f*) Mean normalized *I-V* curves for α1B/β2a/D2 (n = 9), before (*left*) and during (*right*) application of quinpirole. Format and fit function are as in *c*. Before drug application (*left*), $V_{1/2}$ (mV) was 12.9 ± 3.5 and 9.6 ± 3.4, and k (mV) was 4.7 ± 0.1 and 3.6 ± 0.2, in P1 and P2, respectively. During quinpirole application (*right*) $V_{1/2}$ (mV) was 24.8 ± 4.2 and 10.1 ± 3.9, and k (mV) was 7.4 ± 0.4 and 3.9 ± 0.2, in P1 and P2, respectively.

antibodies (Fig. 7 *b*). Fig. 7 *b* shows a single cell transfected with either β1b (*upper left*) or β3 (*lower left*), surrounded by a number of untransfected cells, the presence of which is shown by the nuclear stain (*right*). Immunostaining revealed either very little or no endogenous β subunit protein immunoreactivity in untransfected cells, in contrast to cells

TABLE 1 Influence of quinpirole and a depolarizing prepulse (pp) on I-V parameters

	α1B/D-2 (n = 9)		α1B/β2a/D-2 (n = 9)	
	Shift in $V_{1/2}$ (mV)	Change in k (%)	Shift in $V_{1/2}$ (mV)	Change in k (%)
Influence of quinpirole	+3.3 ± 1.8 (NS)	121.0 ± 10.6 (NS)	+11.9 ± 2.3*	160.7 ± 10.3*
Influence of pp, −quinpirole	−3.3 ± 0.5*	125.4 ± 9.4*	−3.3 ± 0.3*	77.4 ± 4.5*
Influence of pp, +quinpirole	−2.6 ± 2.1 (NS)	112.6 ± 8.6 (NS)	−14.7 ± 1.4*	52.7 ± 3.4*

I-V relations were fitted with a combined Boltzmann and linear fit (see Materials and Methods and Fig. 1) in each experiment. The shifts in $V_{1/2}$ were obtained by subtraction, and the changes in the k factors are presented as a percentage. Increases in the k factor ratio indicate shallower voltage dependence and vice versa.

*Statistically significant difference ($p < 0.05$, Student's t-test).

that were transfected with either β1b or β3. Furthermore, in additional experiments we have found that expression of α1B alone in these cells does not induce the expression of β subunit protein, as evidenced from immunocytochemistry (results not shown). This result is also supported by our previous study, which did not detect endogenous β subunits in COS-7 cells by Western blotting (Campbell et al., 1995a).

DISCUSSION

We have examined the influence of G$\beta\gamma$ dimers and VDCC β subunits, both separately and combined, on the kinetic properties of N-type VDCCs by coexpression with the pore-forming α1B subunits in COS-7 cells. With a VDCC β subunit coexpressed, G protein modulation produced the expected kinetic alterations of the N-type channels (Figs. 1, *b* and *d*; 2; 3, *c* and *d*; 4, *c* and *d*; 5, *b* and *c*; 6, *d–f*), as predicted by a previous model (Patil et al., 1996). In contrast, with no β subunit coexpressed, these kinetic alterations were largely absent (Figs. 1, *a* and *c*; 3, *a* and *b*; 4, *c* and *d*; 5 *a*; 6, *a–c*), although there was still some residual non-voltage-dependent inhibition in this system (Fig. 6 *a*, *bottom*).

The differential coexpression of α1B with either βARK G$\beta\gamma$ binding domain or G$\beta\gamma$ dimers is advantageous because it allows a comparison between G$\beta\gamma$-depleted and saturated populations, respectively. The ensemble average currents obtained here (Fig. 2 *a*) represent the changes in

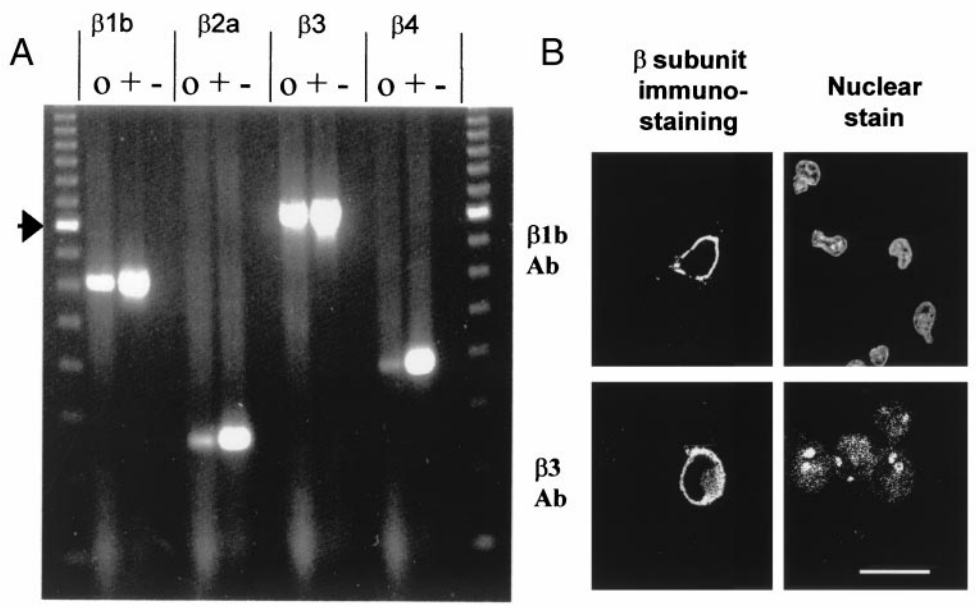

FIGURE 7 Examination of the presence of endogenous VDCC β subunits in COS-7 cells. (*a*) RT-PCR detection of β subunit mRNAs in COS-7 cells. For each β subunit, three lanes are shown: o represents untransfected cells, + represents cells transfected with the specific β subunit, and − represents a negative (H_2O) control. Markers at either side represent a 100-bp ladder; the arrow on the left indicates 800 bp. The details of the primers used are given in the Materials and Methods section. (*b*) Immunostaining for calcium channel β subunits in cells transfected with either β1b (*top*) or β3 (*bottom*). *Left*: A field in which one cell in each case was positively transfected. This shows immunostaining for the specific β subunit; using monoclonal β1b (*upper panel*) or β3 (*lower panel*) antibodies. Untransfected cells present in the same field show little or no immunoreactivity. *Right*: Nuclear staining with the DNA dye YO-YO to show the presence of several cells in each field. The white bar (*bottom right*) represents 10 μm for all panels.

open probability of a single channel. Therefore, it provides a means of "normalization" that could not be achieved with whole-cell current. The whole-cell current can be expressed as current per membrane area (current density), a parameter that still includes the number of channels, which may be affected differentially by the subunit content. The observation of the number of overlapping openings in single/multichannel records allows estimation of the number of channels in the patch and therefore direct comparison between populations transfected with different subunit combinations.

In the experiments in which the dopamine D-2 receptor was coexpressed, the α1B channels are partially tonically modulated because of a certain level of endogenous G$\beta\gamma$, (see Fig. 6, *d* and *e*). The G$\beta\gamma$ level is then further elevated because of receptor activation. In our work, this (receptor-mediated modulation) system had variability and showed some residual inhibition by quinpirole in the absence of expressed VDCC β subunits (Fig. 6). This may reflect the greater complexity of receptor-mediated modulation in activating both voltage-dependent and non-voltage-dependent pathways by multiple signal transduction pathways. However, in general it supports the findings from the former (tonic G$\beta\gamma$ modulation) system, with significantly lower inhibition and lack of significant kinetic slowing or facilitation, when a VDCC β subunit was not coexpressed.

The tonic modulation system provides strongly grounded data showing the role of the VDCC β subunit, both in the suppression by G$\beta\gamma$ of the activation process (Figs. 1, 3 *e*, and 4) and in G$\beta\gamma$ unbinding, as manifested by prepulse facilitation (Figs. 1 *b* and 5). The single-channel data provide strong evidence that the main effect of the β subunit in the βARK1-expressing cells is a twofold increase in the mean open time (compare Fig. 3 *b* with Fig. 3 *d*) and an increase in the activation probability (CFL). The residual effect of G$\beta\gamma$ on α1B expressed without a VDCC β subunit could be partially explained by a reduction in the mean open time (Fig. 3 *b*) or possibly by endogenous VDCC β subunits (Fig. 7 *a*). In contrast, in the presence of a VDCC β subunit it is clear that the activation of α1B was slowed by G$\beta\gamma$, and the number of failures increased (Fig. 4 *c*). To the best of our knowledge, this is the first kinetic examination of both the separate and combined effects of VDCC β subunits and G$\beta\gamma$ dimers.

The role of the auxiliary β subunits in the regulation of N-type channel properties

The involvement of VDCC β subunits in the trafficking of α1 subunits to the plasma membrane is well established (Chien et al., 1995; Brice et al., 1997). Nevertheless, it remains undecided whether they are essential for functional expression. Several groups have provided evidence for β subunit involvement in the modulation of the channel biophysical properties, suggesting interaction with a number of intracellular sites (Stephens et al., 1997; Costantin et al., 1998; Gerster et al., 1999). The different β subunits also have differential effects on inactivation, with β1b, β3, and β4 supporting, and β2a reducing, inactivation (Walker and De Waard, 1998).

Because we wished to avoid the confounding factor of inactivation in our analysis, we used the β2a subunit in most experiments, but broadly similar results were obtained for β1b (Fig. 5). The role of β2a in reducing closed-state inactivation (Patil et al., 1998) is seen here (Fig. 4) as an increase in the maximum opening probability (Imredy and Yue, 1994; Meir et al., 1998), but we made no attempt to study inactivation properties in this study.

Coexpression of the auxiliary β subunit is reported to caused a hyperpolarizing shift in current activation by ~5–10 mV (Wakamori et al., 1999), with no effect on the single-channel conductance (Fig. 3, *b* and *d*). In our hands, only a small nonsignificant shift due to β coexpression was detected in the activation of the whole-cell populations (Fig. 6, *c* and *f*). This may be due to the absence of α2-δ in these experiments, which augments the VDCC β subunit effects (Wakamori et al., 1999). In another study where α1B was cotransfected with α2-δ, using identical Ba^{2+} concentrations to enable direct comparison, a 15-mV hyperpolarizing shift in the activation of the whole-cell current was detected with β subunit coexpression in COS-7 cells (Stephens et al., 2000).

The VDCC β subunit also increased the mean channel open time (Fig. 3, *b* and *d*; $p < 0.05$, Student's *t*-test, for comparison of α1B/βARK versus α1B/β2a/βARK and for α1B/G$\beta\gamma$ versus α1B/β2a/G$\beta\gamma$ at all voltages examined) (Meir et al., 1998; Wakamori et al., 1999). VDCC β2a coexpression enhanced the first opening probability (Fig. 4, *a* and *c*), which is in agreement with improvement of the coupling between gating charge movement and channel opening (Jones et al., 1997).

Because the effects of VDCC β subunit coexpression were significant, and taking into account the immunocytochemistry data on the level of endogenous β subunits, we assume that α1B can be expressed in the membrane without the permanent attachment of this auxiliary subunit. In addition, expression of α1B with an antisense β3 subunit cDNA construct did not prevent the expression of α1B in COS-7 cells (Stephens and Dolphin, unpublished results). However, we cannot entirely discount the possibility that α1B can only be functionally expressed in the plasma membrane with the support of a VDCC β subunit during trafficking.

The effect of auxiliary β2a subunit on the modulation of N-type VDCCs by G$\beta\gamma$

The VDCC α1B/β2a combination, coexpressed with the D-2 receptor, generated currents that were markedly and reversibly inhibited during quinpirole application (Fig. 6 *d*). On the other hand, α1B channels expressed without an

auxiliary β subunit showed much less inhibition, and no slowed activation or enhanced facilitation, when exposed to quinpirole (Fig. 6 *a*). Furthermore, comparison of the single-channel populations formed by α1B when coexpressed with either βARK1 or G$\beta\gamma$ also indicated a much stronger inhibition by G$\beta\gamma$ when VDCC β2a was coexpressed (Fig. 3, *a* and *c*). These findings are supported in our system by kinetic measurements of the response of the α1B channels to moderate voltage steps. The α1B/β2a/G$\beta\gamma$ channels were very slowly activating (Figs. 1 *d* and 3 *e*). In sharp contrast, α1B/Gβ1γ2 currents activated rapidly (Fig. 1 *c*), which would not be expected for modulated channels that are thought to unbind the G$\beta\gamma$ before opening (Patil et al., 1996), with this process being responsible for the slow gating. A marked slowing of the activation process has been proposed to underlie G protein inhibition (Patil et al., 1996) and has been detected in many systems and for several native and heterologously expressed VDCCs (Dolphin, 1995).

The facilitation that is a hallmark of voltage-dependent G protein modulation (Dolphin, 1995) was also strongly dependent on VDCC β subunit coexpression. With β2a, clear facilitation due to a depolarizing prepulse was evident for whole-cell (Stephens et al., 1998) (Figs. 1 *b* and 6, *d* and *e*) and single-channel (Figs. 2–5) currents. With the VDCC β1b subunit coexpressed, a more complex behavior was observed, but clear facilitation (although partially overlaid by inactivation at higher potentials) was also evident (Fig. 5 *c*). The facilitation was time dependent at all voltages (Fig. 5 *b*), involving the addition of a fast G$\beta\gamma$-unbound population to the gating probability. The apparent amount of facilitation for the β2a-containing combinations varied between the different sets of experiments (compare Figs. 1 *b* and 6, *d* and *e*, to Fig. 3 *c, right*). One possible reason for these discrepancies may be the different voltage protocol used for cell-attached (100-ms test pulses and 50-ms prepulse) and whole-cell (50-ms test pulses and 100-ms prepulse) experiments.

Two main questions regarding the role of the VDCC β subunit and G$\beta\gamma$ binding are not answered by the present study. First, as discussed above, can α1 subunits be expressed in the membrane without a chaperoning β subunit (either endogenous or coexpressed)? Second, are α1B channels inhibited to any extent by G$\beta\gamma$ in the absence of the VDCC β subunit? Alternatively, are the effects detected for α1B with no VDCC β subunit coexpressed due solely to a fraction of the channels interacting with endogenous β subunits, allowing the observation of residual inhibition?

While recognizing these limitations, our data strongly support a mechanism in which the VDCC β subunit is necessary for the voltage-dependent modulation of VDCCs. However, this result appears to contradict previous results proposing antagonistic effects of VDCC β subunits on G protein modulation.

Comparison with previous literature: does the VDCC β subunit facilitate or antagonize G$\beta\gamma$ modulation?

Biochemical evidence for overlapping binding sites for auxiliary VDCC β subunit and G$\beta\gamma$ dimers on various α1 subunits (De Waard et al., 1997; Walker et al., 1998, 1999; Canti et al., 1999) suggests a physical basis for an interaction between their effects.

In light of previous results obtained in our laboratory (Campbell et al., 1995b) for native VDCCs in sensory neurons and in other laboratories for *Xenopus* oocytes, we were initially surprised by the lack of G$\beta\gamma$-mediated kinetic slowing in the absence of overexpressed VDCC β subunit. Although our present results do not support the hypothesis of antagonism between β subunits and G$\beta\gamma$ dimers, several explanations may reconcile these apparently contradictory studies.

A number of groups previously reported that the expression of certain β subunits reduced receptor-mediated G protein inhibition of expressed VDCCs (Roche et al., 1995; Bourinet et al., 1996; Qin et al., 1997; Roche and Treistman, 1998a; Canti et al., 1999). Antagonism is supported mainly by recordings from *Xenopus* oocytes, in which an endogenous β3 subunit is active, so that the extent to which the expressed channels represent free α1 subunits is unknown (Tareilus et al., 1997). In the studies cited above, a comparison of the percentage inhibition upon receptor activation showed more inhibition at certain potentials in the absence than in the presence of a coexpressed β subunit. At least part of this effect can be explained by the VDCC β subunit-induced hyperpolarizing shift in current activation, making comparisons of receptor-mediated inhibition at a single potential difficult to interpret. However, facilitation or voltage-dependent relief of inhibition of N-type channels was also enhanced by coexpression of β3, which is similar to the results presented here (Roche and Treistman, 1998b).

In a converse experiment with sensory neurons (Campbell et al., 1995b), VDCC β subunits were partially depleted by an antisense oligonucleotide, and the $GABA_B$-induced inhibition of the native VDCCs was found to be greater in the β subunit-depleted than in control neurons. The reason for the apparent contradiction compared to our present results is unknown, but multiple signaling pathways are activated by G proteins in native neurons, and although G$\beta\gamma$ is widely accepted to be responsible for the voltage-dependent (G$\beta\gamma$-mediated) modulation of N- and P/Q-type channels, voltage-independent modulation has also been described and may be mediated by a number of different pathways (Diverse-Pierluissi et al., 1991; Fitzgerald and Dolphin, 1997). Furthermore, these pathways may also cross-talk with G$\beta\gamma$-mediated voltage-dependent inhibition (Zamponi et al., 1997). Voltage-dependent receptor-mediated inhibition of N-type channels is also influenced by the Gα subunit involved (Kammermeier and Ikeda, 1999). In

our previous study of sensory neurons (Campbell et al., 1995b), we did not examine the proportion of the $GABA_B$-mediated inhibition that was either voltage dependent or voltage independent, and whether this was changed after VDCC β subunit depletion.

In summary, major differences have been observed regarding the amount of inhibition and facilitation of α1B channels in the absence of coexpressed VDCC β subunits between different systems. However, many of these differences may be explained by differences in the endogenous VDCC β subunits, which are low but not absent in the β-antisense-treated sensory neurons and in *Xenopus* oocytes, or by the cellular pathways that are activated by receptor activation or by G protein subunit overexpression in each system. Mechanistically, the apparent contradiction in results and interpretation can also be reconciled by assuming that because of the overlapping or interacting binding sites for G$\beta\gamma$ and VDCC β subunits, the β subunit mainly enhances the depolarization-dependent unbinding of G$\beta\gamma$, which is a form of antagonism. This depolarization-dependent unbinding of G$\beta\gamma$ dimers is thought to underlie most of the voltage-dependent phenomena of G protein modulation. Thus, in the absence of β subunit bound to α1B, no facilitation will occur, and we believe this approximates the case in the present experiments. In contrast, in the presence of a low compared to a high amount of β subunit, as in the *Xenopus* oocytes (and possibly the β-antisense experiments), the main difference may be in the facilitation rate (Roche and Triestman, 1998b) (Canti, Bogdanov and Dolphin, submitted for publication), which represents the rate of G$\beta\gamma$ unbinding during the prepulse. This difference in G$\beta\gamma$ unbinding rate will also manifest itself during the test pulse and result in a greater voltage dependence of inhibition in the presence of exogenous β subunit, which at certain potentials will be observed as a reduction in inhibition (Roche and Triestman, 1998b).

Possible effects of G$\beta\gamma$ on α1B channels

Examination of the effect of G$\beta\gamma$ on α1B channels, with no β subunit cotransfected, reveals shifts of $\sim +5$ mV, in the *I-V*, τ_{act}-*V* (Fig. 1 *c*), and CFL-*V* (Fig. 4 *b*) relationships. In addition, some D-2-transfected cells responded to quinpirole. These small effects may arise from a direct inhibitory effect of G$\beta\gamma$ on α1B, or from some of the α1B channels interacting with endogenous β subunits in COS-7 cells. The latter hypothesis is supported by the presence of endogenous β subunit transcripts detected by RT-PCR in COS-7 cells. It is also supported by the segregation among the responses of cells to D-2 receptor activation (six of 12 and one of 14 cells did not respond to quinpirole, without a VDCC β subunit or with β2a coexpressed, respectively). However, this hypothesis is not supported by the very low level of endogenous β subunit protein compared to that observed when β subunits were transfected into COS-7 cells. Although we have searched for a cell line that does not have endogenous β subunit mRNA, all of the commonly used cell lines (for example, HEK-293) contain β subunit mRNA that is detectable by RT-PCR (data not shown).

Evidence for G$\beta\gamma$ binding directly to the I-II linker of the α1B protein (Dolphin et al., 1999) and other calcium channels (De Waard et al., 1997) strongly suggests that the expressed α1B subunit will bind G$\beta\gamma$ dimers. If G$\beta\gamma$ binds to the α1B subunit in the absence of VDCC β subunit, from our results, the activation of the α1B channel appears to be independent of G$\beta\gamma$ unbinding and may suggest that G$\beta\gamma$ is still associated with the open α1B channel. This is supported mainly by the similar fast activation for α1B/βARK and α1B/G$\beta\gamma$ channels (Fig. 3 *e*) and the lack of facilitation (Figs. 1 *a*, 3 *a*, 4 *a*, 5 *a*) and shorter mean open time (Fig. 3 *b*) for the α1B/G$\beta\gamma$ combination, compared to α1B alone. This hypothesis predicts that with no β subunit, G$\beta\gamma$ is bound to the α1B channel and is either not removed by a depolarizing prepulse or is removed in a much slower fashion. The idea that G$\beta\gamma$-bound "reluctant" channels open and contribute to the modulated current was recently shown for recombinant N-type channels (Colecraft et al., 2000). However, we did not attempt to study the reluctant openings in this system, which may also exist in combinations including the β subunit.

Regulatory mechanisms of the activity-dependent responses of VDCCs in presynaptic nerve terminals and elsewhere include inactivation (Forsythe et al., 1998; Patil et al., 1998), calcium-dependent inactivation (Lee et al., 1999; Peterson et al., 1999), differential subunit interaction (Walker and De Waard, 1998), and neurotransmitter modulation (Dolphin, 1995). Here we have considered the two latter processes and have shown an interaction between these regulatory pathways. The dependence of voltage-dependent G$\beta\gamma$ modulation on the presence of VDCC auxiliary β subunit adds another aspect to the role of the VDCC β subunit in shaping the activity-dependent response of neuronal calcium channels.

We thank Dr. E. Perez-Reyes (Perez-Reyes et al., 1992), Dr T. Snutch, Dr. Y. Mori (Fujita et al., 1993), Dr. H. Chin (Kim et al., 1992), Dr. M. Simon (Fong et al., 1986; Gautam et al., 1989), Dr. S. Moss, and Dr. R. Lefkowitz for gifts of cDNAs. The technical help of Nuria Balaguero and Michelle Li is gratefully acknowledged.

This work was supported by the Wellcome Trust. DCB was an MRC Ph.D. student. We thank Dr. S. Volsen (Eli Lilly, UK) for the β1b and β3 antibodies.

REFERENCES

Bean, B. P. 1989. Neurotransmitter inhibition of neuronal calcium currents by changes in channel voltage-dependence. *Nature.* 340:153–155.

Bogdanov, Y., N. L. Brice, C. Canti, M. J. Page, M. Li, S. G. Volsen, and A. C. Dolphin. 2000. Acidic motif responsible for plasma membrane association of the voltage dependent calcium channel β1b subunit. *Eur. J. Neurosci.* 12:894–902.

Boland, L. M., and B. P. Bean. 1993. Modulation of N-type calcium channels in bullfrog sympathetic neurons by luteinizing hormone-releasing hormone: kinetics and voltage dependence. *J. Neurosci.* 13: 516–533.

Bourinet, E., T. W. Soong, A. Stea, and T. P. Snutch. 1996. Determinants of the G protein-dependent opioid modulation of neuronal calcium channels. *Proc. Natl. Acad. Sci. USA.* 93:1486–1491.

Brice, N. L., N. S. Berrow, V. Campbell, K. M. Page, K. Brickley, I. Tedder, and A. C. Dolphin. 1997. Importance of the different β subunits in the membrane expression of the α1A and α2 calcium channel subunits: studies using a depolarisation-sensitive α1A antibody. *Eur. J. Neurosci.* 9:749–759.

Campbell, V., N. Berrow, K. Brickley, K. Page, R. Wade, and A. C. Dolphin. 1995a. Voltage-dependent calcium channel β-subunits in combination with α_1 subunits have a GTPase activating effect to promote the hydrolysis of GTP by $G\alpha_o$ in rat frontal cortex. *FEBS Lett.* 370:135–140.

Campbell, V., N. S. Berrow, E. M. Fitzgerald, K. Brickley, and A. C. Dolphin. 1995b. Inhibition of the interaction of G protein G_o with calcium channels by the calcium channel β-subunit in rat neurones. *J. Physiol. (Lond.).* 485:365–372.

Canti, C., K. M. Page, G. J. Stephens, and A. C. Dolphin. 1999. Identification of residues in the N-terminus of α1B critical for inhibition of the voltage-dependent-calcium channel by $G\beta\gamma$. *J. Neurosci.* 19: 6855–6864.

Carabelli, V., M. Lovallo, V. Magnelli, H. Zucker, and E. Carbone. 1996. Voltage-dependent modulation of single N-type Ca^{2+} channel kinetics by receptor agonists in IMR32 cells. *Biophys. J.* 70:2144–2154.

Chien, A. J., X. L. Zhao, R. E. Shirokov, T. S. Puri, C. F. Chang, D. Sun, E. Rios, and M. M. Hosey. 1995. Roles of a membrane-localized β subunit in the formation and targeting of functional L-type Ca^{2+} channels. *J. Biol. Chem.* 270:30036–30044.

Colecraft, H. M., P. G. Patil, and D. T. Yue. 2000. Differential occurrence of reluctant openings in G-protein-inhibited N- and P/Q-type calcium channels. *J. Gen. Physiol.* 115:175–192.

Colquhoun, D., and G. H. Hawkes. 1995. The principles of the stochastic interpretation of ion channel mechanisms. *In* Single Channel Recording. B. Sakmann and E. Neher, editors. Plenum, New York. 397–482.

Costantin, J., F. Noceti, N. Qin, X. Y. Wei, L. Birnbaumer, and E. Stefani. 1998. Facilitation by the β_{2a} subunit of pore openings in cardiac Ca^{2+} channels. *J. Physiol. (Lond.).* 507:93–103.

Day, N. C., S. G. Volsen, A. L. McCormack, P. J. Craig, W. Smith, R. E. Beattie, P. J. Shaw, S. B. Ellis, M. M. Harpold, and P. G. Ince. 1998. The expression of voltage-dependent calcium channel beta subunits in human hippocampus. *Mol. Brain Res.* 60:259–269.

De Waard, M., H. Y. Liu, D. Walker, V. E. S. Scott, C. A. Gurnett, and K. P. Campbell. 1997. Direct binding of G-protein βgamma complex to voltage-dependent calcium channels. *Nature.* 385:446–450.

Diverse-Pierluissi, M., K. Dunlap, and E. W. Westhead. 1991. Multiple actions of extracellular ATP on calcium currents in cultured bovine chromaffin cells. *Proc. Natl. Acad. Sci. USA.* 88:1261–1265.

Dolphin, A. C. 1995. Voltage-dependent calcium channels and their modulation by neurotransmitters and G proteins: G. L. Brown prize lecture. *Exp. Physiol.* 80:1–36.

Dolphin, A. C., K. M. Page, N. S. Berrow, G. J. Stephens, and C. Canti. 1999. Dissection of the calcium channel domains responsible for modulation of neuronal voltage-dependent calcium channels by G proteins. *Ann. N.Y. Acad. Sci.* 868:160–174.

Dunlap, K., J. I. Luebke, and T. J. Turner. 1995. Exocytotic Ca^{2+} channels in mammalian central neurons. *Trends Neurosci.* 18:89–98.

Elmslie, K. S., and S. W. Jones. 1994. Concentration dependence of neurotransmitter effects on calcium current kinetics in frog sympathetic neurones. *J. Physiol. (Lond.).* 481:35–46.

Elmslie, K. S., W. Zhou, and S. W. Jones. 1990. LHRH and GTPγS modify calcium current activation in bullfrog sympathetic neurons. *Neuron.* 5:75–80.

Fitzgerald, E. M., and A. C. Dolphin. 1997. Regulation of rat neuronal voltage-dependent calcium channels by endogenous p21-ras. *Eur. J. Neurosci.* 9:1252–1261.

Fong, H. K., J. B. Hurley, R. S. Hopkins, R. Miake-Ley, M. S. Johnson, R. F. Doolittle, and M. I. Simon. 1986. Repetitive segmental structure of the transduction beta subunit: homology with the CDC4 gene and identification of related mRNAs. *Proc. Natl. Acad. Sci. USA.* 83: 2162–2166.

Forsythe, I. D., T. Tsujimoto, M. Barnes-Davies, M. F. Cuttle, and T. Takahashi. 1998. Inactivation of presynaptic calcium current contributes to synaptic depression at a fast central synapse. *Neuron.* 20:797–807.

Fujita, Y., M. Mynlieff, R. T. Dirksen, M.-S. Kim, T. Niidome, J. Nakai, T. Friedrich, N. Iwabe, T. Miyata, T. Furuichi, D. Furutama, K. Mikoshiba, Y. Mori, and K. G. Beam. 1993. Primary structure and functional expression of the ω-conotoxin-sensitive N-type calcium channel from rabbit brain. *Neuron.* 10:585–598.

Gautam, N., M. Baetscher, R. Aebersold, and M. I. Simon. 1989. A G protein γ subunit shares homology with ras proteins. *Science.* 244: 971–974.

Gerster, U., B. Neuhuber, K. Groschner, J. Striessnig, and B. E. Flucher. 1999. Current modulation and membrane targeting of the calcium channel α1C subunit are independent functions of the β subunit. *J. Physiol. (Lond.).* 517:353–368.

Herlitze, S., D. E. Garcia, K. Mackie, B. Hille, T. Scheuer, and W. A. Catterall. 1996. Modulation of Ca^{2+} channels by G-protein βgamma subunits. *Nature.* 380:258–262.

Ikeda, S. R. 1991. Double-pulse calcium channel current facilitation in adult rat sympathetic neurones. *J. Physiol. (Lond.).* 439:181–214.

Ikeda, S. R. 1996. Voltage-dependent modulation of N-type calcium channels by G protein βgamma subunits. *Nature.* 380:255–258.

Imredy, J. P., and D. T. Yue. 1994. Mechanism of Ca^{2+}-sensitive inactivation of L-type Ca^{2+} channels. *Neuron.* 12:1301–1318.

Jones, L. P., P. G. Patil, T. P. Snutch, and D. T. Yue. 1997. G-protein modulation of N-type calcium channel gating current in human embryonic kidney cells (HEK 293). *J. Physiol. (Lond.).* 498:601–610.

Jones, S. W. 1998. Overview of voltage-dependent calcium channels. *J. Bioenerg. Biomembr.* 30:299–312.

Kammermeier, P. J., and S. R. Ikeda. 1999. Expression of RGS2 alters the coupling of metabotropic glutamate receptor 1a to M-type K^+ and N-type Ca^{2+} channels. *Neuron.* 22:819–829.

Kim, H.-L., H. Kim, P. Lee, R. G. King, and H. Chin. 1992. Rat brain expresses an alternatively spliced form of the dihydropyridine-sensitive L-type calcium channel α2 subunit. *Proc. Natl. Acad. Sci. USA.* 89: 3251–3255.

Koch, W. J., J. Inglese, W. C. Stone, and R. J. Lefkowitz. 1993. The binding site for the βgamma subunits of heterotrimeric G proteins on the β-adrenergic receptor kinase. *J. Biol. Chem.* 268:8256–8260.

Lee, A., S. T. Wong, D. Gallagher, B. Li, D. R. Storm, T. Scheuer, and W. A. Catterall. 1999. Ca^{2+}/calmodulin binds to and modulates P/Q-type calcium channels. *Nature.* 399:155–159.

Meir, A., and A. C. Dolphin. 1998. Known calcium channel α1 subunits can form low threshold, small conductance channels, with similarities to native T type channels. *Neuron.* 20:341–351.

Meir, A., E. M. Fitzgerald, and A. C. Dolphin. 1998. Influence of auxiliary subunits on single channel properties of calcium channel α1 subunits co-expressed in COS7 cells. *Soc. Neurosci. Abstr.* 24:1575 (Abstr.).

Meir, A., S. Ginsburg, A. Butkevich, S. G. Kachalsky, I. Kaiserman, R. Ahdut, S. Demirgoren, and R. Rahamimoff. 1999. Ion channels in presynaptic nerve terminals and control of transmitter release. *Physiol. Rev.* 79:1019–1088.

Neher, E. 1995. Voltage Offsets in patch-clamp experiments. *In* Single-Channel Recording. B. Sakmann and E. Neher, editors. Plenum Press, New York. 147–153.

Page, K. M., C. Canti, G. J. Stephens, N. S. Berrow, and A. C. Dolphin. 1998. Identification of the amino terminus of neuronal Ca^{2+} channel α1 subunits α1B and α1E as an essential determinant of G protein modulation. *J. Neurosci.* 18:4815–4824.

Page, K. M., G. J. Stephens, N. S. Berrow, and A. C. Dolphin. 1997. The intracellular loop between domains I and II of the B type calcium channel confers aspects of G protein sensitivity to the E type calcium channel. *J. Neurosci.* 17:1330–1338.

Patil, P. G., D. L. Brody, and D. T. Yue. 1998. Preferential closed-state inactivation of neuronal calcium channels. *Neuron.* 20:1027–1038.

Patil, P. G., M. De Leon, R. R. Reed, S. Dubel, T. P. Snutch, and D. T. Yue. 1996. Elementary events underlying voltage-dependent G-protein inhibition of N-type calcium channels. *Biophys. J.* 71:2509–2521.

Perez-Reyes, E., A. Castellano, H. S. Kim, P. Bertrand, E. Baggstrom, A. E. Lacerda, X. Wei, and L. Birnbaumer. 1992. Cloning and expression of a cardiac/brain β subunit of the L-type calcium channel. *J. Biol. Chem.* 267:1792–1797.

Peterson, B. Z., C. D. De Maria, and D. T. Yue. 1999. Calmodulin is the Ca^{2+} sensor for Ca^{2+}-dependent inactivation of L-type calcium channels. *Neuron.* 22:542–558.

Qin, N., D. Platano, R. Olcese, E. Stefani, and L. Birnbaumer. 1997. Direct interaction of Gβgamma with a C-terminal Gβgamma binding domain of the calcium channel α1 subunit is responsible for channel inhibition by G protein coupled receptors. *Proc. Natl. Acad. Sci. USA.* 94: 8866–8871.

Roche, J. P., V. Anantharam, and S. N. Treistman. 1995. Abolition of G protein inhibition of α_{1A} and α_{1B} calcium channels by co-expression of the β_3 subunit. *FEBS Lett.* 371:43–46.

Roche, J. P., and S. N. Treistman. 1998a. The Ca^{2+} channel β_3 subunit differentially modulates G-protein sensitivity of α_{1A} and α_{1B} Ca^{2+} channels. *J. Neurosci.* 18:878–886.

Roche, J. P., and S. N. Treistman. 1998b. Ca^{2+} channel β3 subunit enhances voltage-dependent relief of G-protein inhibition induced by muscarinic receptor activation and G$\beta\gamma$. *J. Neurosci.* 18:4883–4890.

Stephens, G. J., N. L. Brice, N. S. Berrow, and A. C. Dolphin. 1998. Facilitation of rabbit α1B calcium channels: involvement of endogenous Gβgamma subunits. *J. Physiol. (Lond.).* 509:15–27.

Stephens, G. J., K. M. Page, Y. Bogdanov, and A. C. Dolphin. 2000. The α1B calcium channel amino terminus contributes determinants for β subunit mediated voltage-dependent inactivation properties. *J. Physiol. (Lond.).* 525:377–390.

Stephens, G. J., K. M. Page, J. R. Burley, N. S. Berrow, and A. C. Dolphin. 1997. Functional expression of rat brain cloned α1E calcium channels in COS-7 cells. *Pflügers Arch.* 433:523–532.

Tareilus, E., M. Roux, N. Qin, R. Olcese, J. M. Zhou, E. Stefani, and L. Birnbaumer. 1997. A *Xenopus* oocyte β subunit: evidence for a role in the assembly/expression of voltage-gated calcium channels that is separate from its role as a regulatory subunit. *Proc. Natl. Acad. Sci. USA.* 94:1703–1708.

Tsien, R. W., P. T. Ellinor, and W. A. Horne. 1991. Molecular diversity of voltage-dependent Ca^{2+} channels. *Trends Pharmacol. Sci.* 12:349–354.

Wakamori, M., G. Mikala, and Y. Mori. 1999. Auxiliary subunits operate as a molecular switch in determining gating behaviour of the unitary N-type Ca^{2+} channel current in *Xenopus* oocytes. *J. Physiol. (Lond.).* 517:659–672.

Walker, D., D. Bichet, K. P. Campbell, and M. De Waard. 1998. A β_4 isoform-specific interaction site in the carboxyl-terminal region of the voltage-dependent Ca^{2+} channel α_{1A} subunit. *J. Biol. Chem.* 273: 2361–2367.

Walker, D., D. Bichet, S. Geib, E. Mori, V. Cornet, T. P. Snutch, Y. Mori, and M. De Waard. 1999. A new beta subtype-specific interaction in alpha1A subunit controls P/Q-type Ca^{2+} channel activation. *J. Biol. Chem.* 274:12383–12390.

Walker, D., and M. De Waard. 1998. Subunit interaction sites in voltage-dependent Ca^{2+} channels. *Trends Neurosci.* 21:148–154.

Zamponi, G. W., E. Bourinet, D. Nelson, J. Nargeot, and T. P. Snutch. 1997. Crosstalk between G proteins and protein kinase C mediated by the calcium channel α_1 subunit. *Nature.* 385:442–446.

Zamponi, G. W., and T. P. Snutch. 1998. Decay of prepulse facilitation of N type calcium channels during G protein inhibition is consistent with binding of a single $G_{\beta gamma}$ subunit. *Proc. Natl. Acad. Sci. USA.* 95: 4035–4039.